

Exciton-Plasmon-Photon Conversion in Plasmonic Nanostructures

Y. Fedutik, V. V. Temnov, O. Schöps, and U. Woggon*

Fachbereich Physik, Universität Dortmund, Otto-Hahn-Strasse 4, 44227 Dortmund, Germany

M. V. Artemyev

Institute for Physico-Chemical Problems, Belarussian State University, Minsk 220080, Belarus

(Received 21 June 2007; published 24 September 2007)

A silver-nanowire cavity is functionalized with CdSe nanocrystals and optimized towards cavity quantum electrodynamics by varying the nanocrystal-nanowire distance d and cavity length L . From the modulation of the nanocrystal emission by the cavity modes a plasmon group velocity of $v_{gr} \sim 0.5c$ is derived. Efficient exciton-plasmon-photon conversion and guiding is demonstrated along with a modification in the spontaneous emission rate of the coupled exciton-plasmon system.

DOI: 10.1103/PhysRevLett.99.136802

PACS numbers: 73.20.Mf, 42.50.-p, 42.60.Da, 73.22.-f

The quantum optical coupling between electronic states and photons is of fundamental interest and intensively investigated in such prominent systems as single atoms in traps or semiconductor quantum dots in optical microcavities [1–6]. Such model systems allow us to study strong exciton-photon coupling and atom-photon entanglement, photon statistics, and many other fundamental phenomena of cavity quantum electrodynamics (cavity-QED). An open and widely discussed question is whether exciton-plasmon interactions are suitable to study fundamental quantum optical phenomena. Theoretical concepts propose plasmonic nanocavities as test structures for studies of superradiance, surface-plasmon-supported photon coherence, or surface plasmon amplification by stimulated emission of radiation (spaser) [7–10]. The demonstration of enhanced spontaneous emission of nanoscaled optical emitters, e.g., molecules or nanocrystals, near metallic surfaces, colloidal gold particles, or metallic tips [11–23] represents a strong motivation to explore further quantum optical phenomena in plasmonic nanocavities. While metal wires or nanoshells are discussed as examples for passive plasmonic nanocavities [24–29], optically active plasmonic cavities, i.e., functionalized with nanoscale emitters, are less studied.

In this Letter we report about a metal-isolator-semiconductor multishell system which unifies the local effect of enhanced spontaneous emission due to a modified density of states near metallic nanostructures with the excitation of surface plasmons (SPs) and their propagation in a 1D-nanowire resonator. Such a prototype for an active plasmonic nanocavity allows us to operate and control exciton-plasmon-photon conversion as well as the guiding of electromagnetic waves on a nanoscale. The composite nanosystem we present here consists of a wet-chemically grown Ag-wire core (100–200 nm in diameter, length between 4 and 40 μm) which is covered by a SiO_2 shell of different, well-defined thickness d followed by an outer shell of homogeneously distributed, highly luminescent CdSe nanocrystals (NCs) [30]. Figure 1 illustrates the

basic operation principles of the proposed plasmonic nanoresonator.

To create such a structure in reality, several conceptual steps in cavity design are necessary which we illustrate in the following with Fig. 2. In the first step the thickness d of a dielectric SiO_2 layer has to be optimized to achieve the maximum possible exciton-plasmon conversion efficiency. For this purpose the exciton-plasmon interaction has been investigated on individual multishell nanowires by microphotoluminescence imaging spectroscopy ($\mu\text{-PL}$) at the diffraction limit using an imaging spectrometer combined with a cooled CCD camera. An example of such a measurement is shown in Fig. 2, where we compare the $\mu\text{-PL}$ images of a CdSe NCs/ SiO_2 /Ag nanowire [Figs. 2(a), 2(c), and 2(e)] with the PL intensity of a hollow CdSe NCs/ SiO_2 reference sample where the Ag core was dissolved in ammonia [Figs. 2(b) and 2(d)]. The single nanowires were spatially homogeneously excited with a

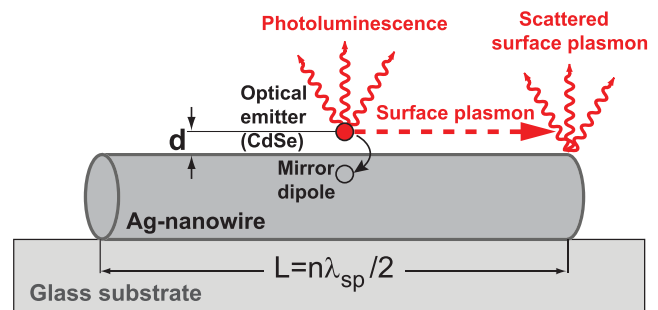


FIG. 1 (color). Plasmonic nanocavity consisting of a metallic (Ag) nanowire functionalized by optical emitters (CdSe nanocrystals) on top of a dielectric (SiO_2) shell of thickness d . The excited optical emitters have three channels for energy relaxation [12]: photoluminescence (PL) into free space, dipole-dipole interaction with the damped mirror dipole (also called “lossy surface waves”), excitation of surface plasmons and plasmon-photon-conversion as the result of scattering at surface roughnesses (low efficiency) and structural discontinuities such as the Ag-nanowire ends (high efficiency).

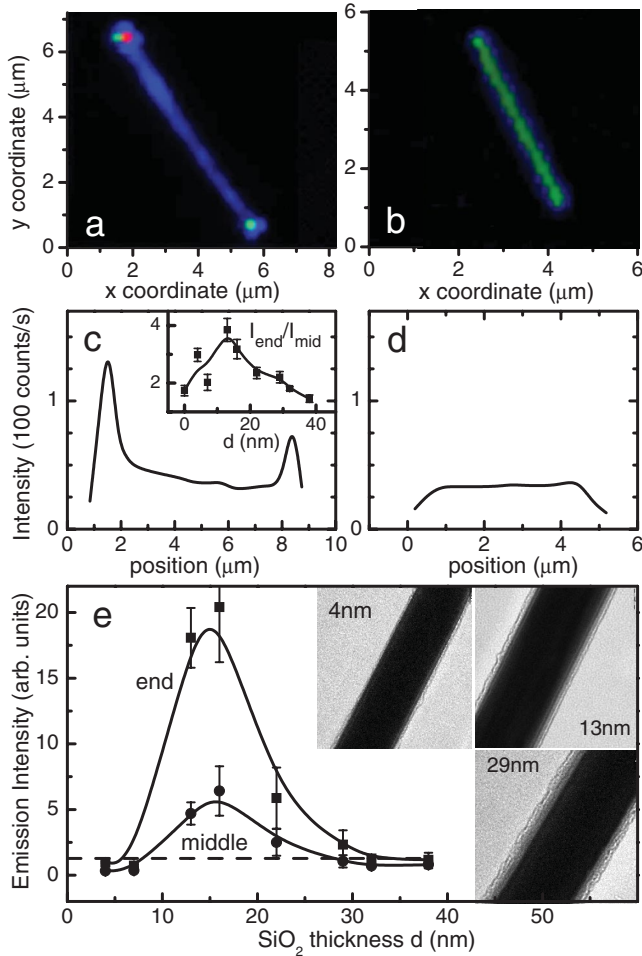


FIG. 2 (color). (a) μ -PL image of the 635 nm CdSe NC emission for a $7.5 \mu\text{m}$ long multishell Ag nanowire with a SiO_2 shell of 22 nm; (b) the same for a hollow CdSe NCs- SiO_2 shell system of $\sim 4 \mu\text{m}$ length after dissolving the inner Ag core. (c),(d) The spatially resolved emission intensity measured along the nanowire axis with (c) and without (d) Ag core. The inset of (c) shows the ratio of the emission intensity measured for the nanowire end and middle part $I_{\text{end}}/I_{\text{mid}}$ as a function of SiO_2 shell thickness d . (e) NC emission intensity measured at the multishell nanowire middle and end as a function of shell thickness d . Dashed line: NC emission on a hollow SiO_2 shell. $\lambda_{\text{pump}} = 532 \text{ nm}$, pump power 60 mW, spot size $30 \mu\text{m}$, $T = 300 \text{ K}$. Inset: TEM images as examples for three wires with diameter of 120 nm and SiO_2 shell thickness of 4, 13, and 29 nm, respectively.

moderate cw-pump power of up to $10 \text{ kW}/\text{cm}^2$ resonant to the NC excited state absorption band [31]. Whereas the metal-free reference sample shows a spatially homogeneous emission profile [32], the CdSe NCs/ SiO_2 /Ag sample exhibits pronounced intensity maxima at the nanowire ends, which is the first hint of Ag-nanowire SP excitation via NC exciton emission. In order to optimize the NC-SP coupling efficiency of the CdSe NCs/ SiO_2 /Ag sample, the thickness d of the SiO_2 shell has been systematically varied. Figure 2(e) shows the dependence of the emission

intensity for individual nanowires with different shell thickness d spatially resolved in the middle and at the end of the wire. The dashed horizontal line in Fig. 2(e) indicates the PL intensity of a metal-free CdSe NCs/ SiO_2 reference sample. The observed dependence of the CdSe/ SiO_2 /Ag-nanowire emission intensity on d is the result of the competition of different energy relaxation mechanisms caused by the vicinity of a metallic core as sketched in Fig. 1. For small d , well below 10 nm, the emission is strongly suppressed (PL quenching), in agreement with the expected dominance of the dipole-dipole interaction with the damped mirror dipole [12]. An enhancement of the NC emission is found for a SiO_2 shell thickness of $d \approx 15 \text{ nm}$ in agreement with recent experiments on layers of colloidal gold nanoparticles [14]. We assign the observed emission enhancement at that SiO_2 thickness d to a combination of a change in the NC spontaneous emission rate caused by the modified density of states near metallic surfaces or nanostructures and a contribution from residual scattering of Ag SPs on the nanowire surface discontinuities (see Fig. 1). The role of surface roughness in similar experiments was recently emphasized, e.g., in [15,23]. The found maximum emission enhancement at a NC-metal distance of $d \approx 15 \text{ nm}$ is in very good agreement with theoretical predictions made by Ford and Weber [12] for the electromagnetic interaction of molecules with flat metal surfaces. Their calculations yield a maximum in the total decay rate at a distance d of 30 nm to the silver surface for parallel to the surface oriented dipoles. In qualitative agreement are also recent observations of a strong emission enhancement in the close vicinity of a spherical metal nanoparticle [33,34]. In addition to the maximum around 15 nm, we see in Fig. 2(e) a decrease of the emission intensity with further increasing d , which is an interesting observation and the subject of further investigations.

The emission from the nanowire tips, where the plasmon-photon coupling efficiency is expected to be much higher as compared to that caused by the residual surface roughness in the middle of the nanowire, shows a remarkably stronger dependence on d [Fig. 2(e)] on which we will focus in the following. Plotting the ratio of the emission intensity of the nanowire end and middle part $I_{\text{end}}/I_{\text{mid}}$ versus SiO_2 shell thickness d we found again the maximum around 15 nm [see the inset of Fig. 2(c)]. However, even for small and large d we still have stronger emission at the nanowire ends compared to the middle. This fact is either due to electric-field enhancement at geometrical wire discontinuities at the nanowire ends or due to SP transport towards the ends after NC exciton—Ag plasmon conversion across the full wire followed by SP propagation. We strongly favor the latter explanation and will present below the supporting arguments.

According to our model sketched in Fig. 1, the plasmonic nanostructure has to show (i) an enhancement of the spontaneous emission rate, (ii) the saturation of the emission intensity at the nanowire ends with increasing nano-

wire length caused by the finite plasmon propagation length L_{SP} , and (iii) the Fabry-Perot-like modulation of the nanocrystal emission spectrum as an indication of multiple reflections of the surface plasmons from the nanowire ends.

Figure 3 shows the emission dynamics of the coupled exciton-plasmon system, excited by femtosecond pulses of a frequency-doubled Ti:sapphire laser, measured at single multishell nanowires of about $15 \mu\text{m}$ length by a streak camera at 635 nm, the maximum of the CdSe NC spectrum. The decay curves are highly nonexponential due to a complex combination of radiative and nonradiative decay rates. For simplicity, and to discuss only qualitatively the d sensitivity of the radiative component in the decay dynamics, all curves are fitted by two exponential decay rates $I(t) \sim A_1 \exp(-t/\tau_1) + A_2 \exp(-t/\tau_2)$ (taking into account the finite instrumental response shown as a dashed line in Fig. 3). The long decay time τ_2 of a few nanoseconds is similar for all samples and can most likely be attributed to the recombination of exciton states of uncoupled or less-coupled NCs. That long decay component is not very sensitive to d . In contrast, the fast initial decay appears to be sensitive to d (see Fig. 3). A fit of the early dynamics of the multishell nanowire sample with large spacer thickness ($30 < d < 40 \text{ nm}$) yields an initial decay time of $\tau_1 = 38 \text{ ps}$ with an amplitude $A_1 = 0.69$. The multishell nanowire with the optimum spacer thickness as derived from Fig. 2(e) with $12 < d < 18 \text{ nm}$ exhibits a distinctly faster initial decay with a decay time of 16 ps and $A_1 = 0.88$. Thus, in agreement with the enhancement of emission intensity shown in Fig. 2, we observe a consistent enhancement in the nanocrystal emission dynamics which we assign to a change of predominantly the radiative part

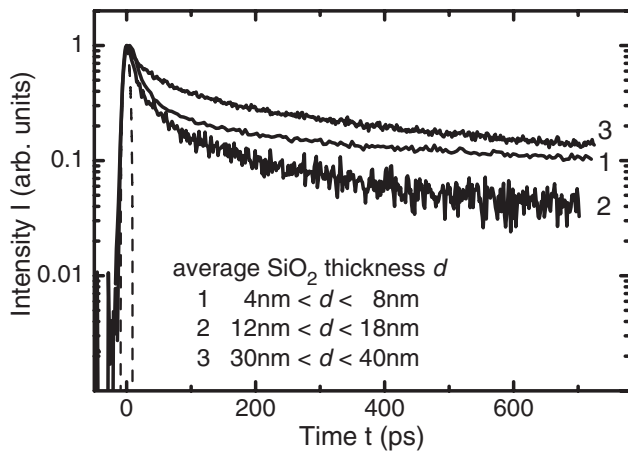


FIG. 3. Emission dynamics of single multishell Ag nanowire of $L \approx 15 \mu\text{m}$ for different SiO_2 shell thicknesses. For the fast initial decay the decay times of 20 ps for sample 1, 16 ps for sample 2, and 38 ps for sample 3 have been extracted. The dashed line shows the instrumental response to the laser pulse with a 10 ps time resolution. $\lambda_{\text{pump}} = 409 \text{ nm}$, $\tau_{\text{pulse}} = 150 \text{ fs}$, $T = 300 \text{ K}$.

of the overall decay. The multishell nanowire with very thin shells ($4 < d < 8 \text{ nm}$) shows $\tau_1 = 20 \text{ ps}$ and $A_1 = 0.91$. For this latter sample, the interpretation of the experimental data is difficult since the weak signal of predominantly nonradiatively decaying, i.e., quenched NCs, might have contributions from weak background emission of unbound NCs. In addition, for small d the NCs are still sensitive to atomic layer fluctuations or small clusters at the silver-nanowire surface which may support a local emission enhancement effect. Note that for all studied nanoresonators the cavity Q factor is still far below such values needed to affect the spontaneous emission enhancement.

To investigate the nanocrystal-initiated plasmon excitation and propagation, we analyze in Fig. 4 the ratio of the emission intensity $I_{\text{end}}/I_{\text{mid}}$ as a function of Ag wire length L . The observed saturation behavior for $I_{\text{end}}/I_{\text{mid}}$ is caused by the damping of the plasmon propagation along the 1D nanowire. The saturation data of $I_{\text{end}}/I_{\text{mid}}$ when increasing L can be used to estimate the plasmon propagation length L_{SP} for different NC emission wavelengths by shifting and squeezing the curves to a normalized intensity range from 0 to 1 and fitting the asymptotic behavior by the function $I = [1 - \exp(-L/L_{SP})]$. The result of the best fitting is shown in the inset of Fig. 4 which yields the plasmon propagation lengths in silver nanowires to $7 \mu\text{m}$ for 545 nm, $11 \mu\text{m}$ for 595 nm, $12 \mu\text{m}$ for 605 nm, $13 \mu\text{m}$ for 635 nm, and $30 \mu\text{m}$ for 809 nm. The obtained spectral dependence of L_{SP} is in good qualitative agreement with the reported data about plasmon propagation on silver surfaces [35–37]. The length L_{SP} represents the typical limit for the nanowire length L which allows for back-reflection and the buildup of surface plasmon standing wave cavity modes.

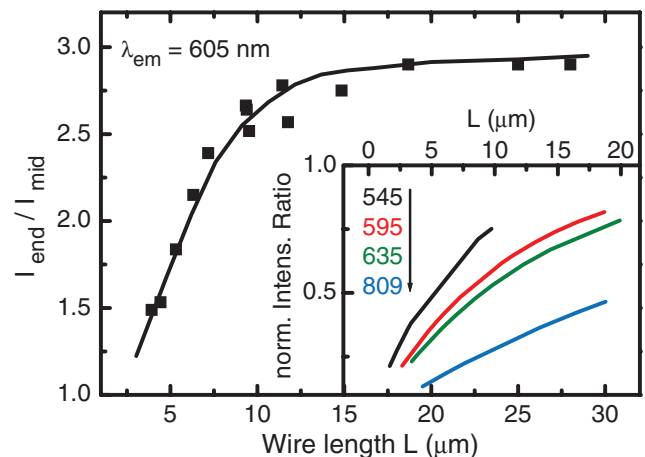


FIG. 4 (color). Ratio of the emission intensity $I_{\text{end}}/I_{\text{mid}}$ as a function of wire length L and NC emission wavelength. Squares: Data for CdSe nanorods with PL maximum at 605 nm. Inset: Experimental fits (see text) of the normalized intensity ratio for different CdSe NCs with PL maxima at 545, 595, 635 nm and CdTe at 809 nm. $\lambda_{\text{pump}} = 488 \text{ nm}$, $T = 300 \text{ K}$.

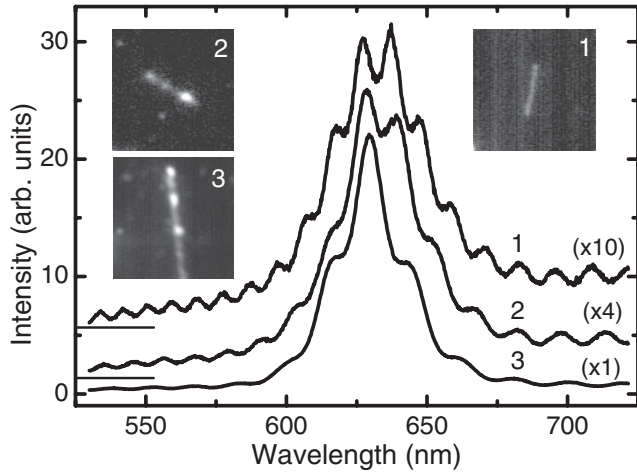


FIG. 5. Nanocrystal emission spectra modulated by the silver nanocavity modes measured for silver wires of different length L and a SiO_2 shell of $d = 10\text{--}15$ nm. Wire 1 and wire 2 are almost defect free with $L = 9.7\ \mu\text{m}$ and $L = 8.8\ \mu\text{m}$. Wire 3 couples plasmons into free space photons at a defect at $L \approx 6.6\ \mu\text{m}$. From the period of the spectral modulations a group velocity of $v_g \approx 0.5c$ is derived for the silver wire plasmon demonstrating the direct coupling of nanocrystal photons to plasmons of the Ag wire. $\lambda_{\text{pump}} = 488$ nm, $T = 300$ K.

After the demonstration of efficient exciton-plasmon-photon conversion, we show finally that the CdSe NC emission spectra can become modulated by the nanocavity modes. Longitudinal cavity modes exist whenever an integer of half the surface plasmon wavelength equals the wire length (see Fig. 1). With Fig. 5 we show some examples for emission spectra of multishell nanowires taken at the nanowire ends and/or structural defects (bright spots in the nanowire images shown in the inset). Wires 1 and 2 are almost defect free with $L = 9.7\ \mu\text{m}$ and $L = 8.8\ \mu\text{m}$ while wire 3 couples plasmons into free space photons at a defect at $L \approx 6.6\ \mu\text{m}$. The longest resonator (wire 1) shows the shortest modulation period of $\Delta\lambda \approx 10.5$ nm at ~ 650 nm while the shortest resonator (wire 3) has the largest modulation period of $\Delta\lambda \approx 14.3$ nm. From the period of the spectral modulations of wires 1, 2, and 3 a surface plasmon group velocity of $v_{\text{gr}} = 2cL(\Delta\lambda/\lambda^2) \approx (0.5 \pm 0.1)c$ can be extracted for silver nanowires [38], in quantitative agreement with previously reported results [27] and demonstrating the direct coupling of nanocrystal photons to plasmons of the Ag wire.

To summarize, we reported about the experimental realization of a 1D-plasmonic nanocavity consisting of a single Ag nanowire functionalized with CdSe NCs on top of a 15 nm thin SiO_2 -spacer layer. Despite the very low and far from being optimized quality factor of that plasmonic nanocavity, the system presented here is an interesting candidate to explore such phenomena as collective spontaneous emission into a single plasmon mode (super-

radiance), photon statistics, and temporal coherence properties of the emission in weakly coupled exciton-plasmon systems.

*ulrike.woggon@uni-dortmund.de

- [1] R.J. Thompson *et al.*, Phys. Rev. Lett. **68**, 1132 (1992).
- [2] M. Brune *et al.*, Phys. Rev. Lett. **76**, 1800 (1996).
- [3] J.P. Reithmaier *et al.*, Nature (London) **432**, 197 (2004).
- [4] T. Yoshie *et al.*, Nature (London) **432**, 200 (2004).
- [5] E. Peter *et al.*, Phys. Rev. Lett. **95**, 067401 (2005).
- [6] N. Le Thomas *et al.*, Nano Lett. **6**, 557 (2006).
- [7] V. V. Temnov and U. Woggon, Phys. Rev. Lett. **95**, 243602 (2005).
- [8] D. E. Chang *et al.*, Phys. Rev. Lett. **97**, 053002 (2006).
- [9] Choon How Gan *et al.*, Phys. Rev. Lett. **98**, 043908 (2007).
- [10] D.J. Bergman and M.I. Stockman, Phys. Rev. Lett. **90**, 027402 (2003).
- [11] K. H. Drexhage, J. Lumin. **1/2**, 693 (1970).
- [12] G. W. Ford and W. H. Weber, Phys. Rep. **113**, 195 (1984).
- [13] L. Novotny *et al.*, Phys. Rev. Lett. **86**, 5251 (2001).
- [14] O. Kulakovich *et al.*, Nano Lett. **2**, 1449 (2002).
- [15] K. T. Shimizu *et al.*, Phys. Rev. Lett. **89**, 117401 (2002).
- [16] E. Dulkeith *et al.*, Phys. Rev. Lett. **89**, 203002 (2002).
- [17] C. Sönnichsen *et al.*, Phys. Rev. Lett. **88**, 077402 (2002).
- [18] Jaebeom Lee *et al.*, Nano Lett. **4**, 2323 (2004).
- [19] J.R. Lakowicz, Anal. Biochem. **337**, 171 (2005).
- [20] I. Gryczynski *et al.*, J. Phys. Chem. B **109**, 1088 (2005).
- [21] B. C. Buchler *et al.*, Phys. Rev. Lett. **95**, 063003 (2005).
- [22] J. Kalkman *et al.*, Appl. Phys. Lett. **86**, 041113 (2005).
- [23] K. Okamoto, S. Vyawahare, and A. Scherer, J. Opt. Soc. Am. B **23**, 1674 (2006).
- [24] J. C. Weeber *et al.*, Phys. Rev. B **60**, 9061 (1999).
- [25] S. Coyle *et al.*, Phys. Rev. Lett. **87**, 176801 (2001).
- [26] E. Prodan *et al.*, Nano Lett. **3**, 1411 (2003).
- [27] H. Ditlbacher *et al.*, Phys. Rev. Lett. **95**, 257403 (2005).
- [28] R. M. Dickson and L. A. Lyon, J. Phys. Chem. B **104**, 6095 (2000).
- [29] A. Bouhelier *et al.*, Phys. Rev. Lett. **95**, 267405 (2005).
- [30] The chemical preparation will be reported elsewhere.
- [31] The direct laser excitation and propagation of Ag-SPs is suppressed by the blue-green excitation wavelength for which $L_{\text{SP}} \ll L$. The polarization of the exciting laser is perpendicular to the nanowire axis so that the direct excitation of Ag-SPs is forbidden.
- [32] The nanocrystal emission taken from the hollow CdSe NCs/ SiO_2 nanowire reference sample did not show distinct differences when exciting with different polarizations of the exciting lasers indicating a random orientation of the nanocrystal dipoles.
- [33] P. Anger *et al.*, Phys. Rev. Lett. **96**, 113002 (2006).
- [34] S. Kühn *et al.*, Phys. Rev. Lett. **97**, 017402 (2006).
- [35] P. Dawson *et al.*, Phys. Rev. Lett. **72**, 2927 (1994).
- [36] B. Lamprecht *et al.*, Appl. Phys. Lett. **79**, 51 (2001).
- [37] A. Bouhelier and G.P. Wiederrecht, Phys. Rev. B **71**, 195406 (2005).
- [38] V. V. Temnov *et al.*, Opt. Lett. **32**, 1235 (2007).